SEMARAK ILMU PUBLISHING

Journal of Advanced Research in Fluid Mechanics and Thermal Sciences

Journal homepage:
https://semarakilmu.com.my/journals/index.php/fluid_mechanics_thermal_sciences/index
ISSN: 2289-7879

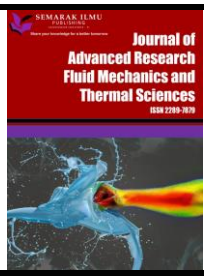

Mathematical Modeling and Validation of Solar-Induced Ventilation System for Vehicle Cabin Cooling in Hot Parking Conditions

Adel Abulgasm Lahimer[1,4], Amir Abdul Razak[1,2,3,*], Kamaruzzaman Sopian[5]

[1] Energy Sustainability Focus Group (ESFG), Faculty of Mechanical & Automotive Engineering Technology, Universiti Malaysia Pahang, Malaysia
[2] Centre for Advanced Industrial Technology (AIT), Universiti Malaysia Pahang Al-Sultan Abdullah, 26600 Pekan Pahang, Malaysia
[3] Pusat Kelestarian Ekosistem dan Sumber Alam (ALAM), Universiti Malaysia Pahang Al-Sultan Abdullah, 26600 Pekan Pahang, Malaysia
[4] Research Center and Manufacturing, Benghazi, Libya
[5] Department of Mechanical Engineering, Universiti Teknologi PETRONAS, Malaysia

ARTICLE INFO

Article history:
Received 15 July 2023
Received in revised form 13 September 2023
Accepted 24 September 2023
Available online 14 October 2023

Keywords:
Solar chimney; mathematical model validation; passive cooling; natural ventilation; vehicle cabin soak temperature reduction

ABSTRACT

Exposure to direct sunlight raises interior temperatures in vehicle cabins, risking heat-related illnesses. Solar passive techniques mitigate this issue, especially during hot parking conditions. However, a comprehensive mathematical model encompassing both solar chimney and vehicle cabin is lacking. This study develops a novel mathematical model to predict temperature distribution and airflow rate, enhancing system performance evaluation. The system comprises a solar air collector with an adjustable arm mounted on the vehicle's roof. The model was validated theoretically and experimentally. The experimental work is conducted with the physical model with an air gap of 0.1 m, 0.77 m width, and a 1.12 m collector length under outdoor conditions. Results indicated a gradual increase in temperatures of the glass cover, air in the collector channel, absorber, and mass airflow rate with solar radiation intensity, significantly influencing system performance. The high value of R2 and the consistency of the model's results with theoretical and experimental outcomes justified the validity and accuracy of the proposed model, exhibiting a deviation percentage of less than 10%. The developed model can be utilized to study influential parameters for optimizing the proposed strategy's performance and components, yielding comparable results to experimental data. Additionally, it provides researchers and car makers with a broader perspective and a range of options for further improvement in weight, size, cost, and aerodynamic of the vehicle.

1. Introduction

Developing approaches to decrease the high interior cabin soak air temperature for realizing human thermal comfort, decreasing peak cooling load and cooling capacity for improving fuel economy, and reducing tailpipe emissions have been of significant interest to car-makers and researchers since the vehicles have been on the road.

* *Corresponding author.*
E-mail address: amirrazak@umpsa.edu.my

https://doi.org/10.37934/arfmts.110.1.200226

Replacing the interior cabin air of a soaked parked car instantaneously with fresh ambient air using passive cooling techniques can be considered a practical approach to reduce the high cabin air temperature and improve the human comfort level upon entry. A solar-powered ventilator is the most common technique extensively studied in this field. For example, using photovoltaic power ventilation to reduce interior cabin temperature has been examined by Chiou [1]. On the other hand, some researchers reported that the solar-powered auto air ventilator's performance was never proven efficient due to its low flow rate and minimal reduction in the interior surfaces' temperatures [2]. Also, their application is impractical since the car windows must be rolled down a few centimeters to fit the ventilators, and the user requires placing the ventilator on the window each time (time-consuming) [2,3]. Besides, its application is unsuitable for window-tinted cars because tints will decrease solar panels' solar energy absorption [2]. However, passive cooling from an approach that uses solar energy to induce natural ventilation for enhancing cabin thermal comfort and fuel economy under hot soaking conditions can be obtained from a solar chimney which demonstrated promising results in reducing the peak cabin soak temperature (20.5°C), as reported in Lahimer *et al.,* [4].

Although cooling a hot compartment of a soaked vehicle using different passive approaches has been studied extensively in the literature, a mathematical model for incorporating the solar chimney as a solar passive approach on vehicle cabin roofs has not been reported in the relevant literature or studies. This study is the first attempt to develop a model to incorporate them.

There will be many critical achievements from the development of this model; for example, the proposed model will allow researchers to evaluate and identify the potential and limitations of the solar-induced ventilation system for cabin temperature reduction. In addition, the model can be used to optimize the system thermal performance for promoting the passive cooling strategy for temperature reduction of a vehicle soaked under the direct sun. In this paper, the following objectives are sought after:

(i) To develop a comprehensive mathematical model incorporating a solar-induced ventilation system into the roof of a vehicle cabin for energy analysis and parametric studies for obtaining the optimum geometries and performance for optimization and designing of the solar chimney.
(ii) To validate the developed model theoretically and experimentally to justify the proposed model's validity and accuracy.
(iii) To comprehensively evaluate the fundamental behavior and the heat transfer interaction for every component that constructs the proposed system.

1.1 Principles and Applications

Utilizing solar energy to generate sufficient temperature differences with the environment has been employed globally for centuries for power generation, space ventilation, and in agriculture for air replacement in greenhouses and drying crops [5-10]. The solar chimney is the most widely used device as a practical passive technique to generate airflow through the occupied space to provide cooling and enhance the space's natural ventilation [11,12]. Another kind of solar chimney is a solar heated chimney or solar roof chimney, which consists of the collector with or without stack and can be defined as a natural thermal pump that utilizes solar energy, which functions as an air-moving device for space heating, ventilation, and cooling. In addition, solar roof chimneys can be combined with other passive approaches such as the evaporative cooling technique, solid adsorption cooling cavity, and ground-to-air heat exchanger to enhance the internal thermal environment and air quality to improve human thermal comfort.

The principal driving mechanism of airflow through the chimney channel is thermal buoyancy force or temperature force due to changes in air density [13]. Thus, the primary function of the solar chimney is to feed the density variation along the collector channel to generate enough draft to overcome the negative thermal gravity effect under the design mass airflow [14,15].

Till now, there has been increasing interest in re-employing solar chimney principles for different applications in different fields, for example, integrating solar chimney power systems with seawater desalination to produce electricity and freshwater [16]. Recently, Lahimer *et al.,* [4] introduced the solar chimney concept as a promising passive approach for cabin soak temperature reduction.

1.2 Modeling Work

Bansal *et al.,* [6] developed the first mathematical model for an inclined solar chimney derived from classical energy balance equations for a steady-state for enhanced stack ventilation. Andersen [17] presented a mathematical approach to predict the natural ventilation in a room with small openings by a set of equations based on the pressure model. Hirunlabh *et al.,* [18] developed a mathematical model to study the effect of height and air gap on the performance of a metallic solar wall. Their validation showed a good agreement between the mathematical predictions and experimental results. Afonso and Oliveira [19] developed a thermal model and transient simulation considering the unsteady state one-dimensional heat transfer mode in the direction of the brick wall, pressure losses between the inlet and outlet, friction losses in the chimney walls, heat storage in the chimney walls, and wind effect. Their results showed that the airflow rate increased with the increase in the solar chimney height and linearly with the increase in the width and flow section. Ong [20] presented a mathematical model for a vertical non-metallic solar chimney to study the thermal performance of the solar chimney. It was found that the air mass flow rate increases correspond to the increase of wall length or solar radiation. Their simulation data were validated against Hirunlabh *et al.,* [18] experimental results and correlated satisfactorily. Dai *et al.,* [21] developed a mathematical model without considering the wind effect to predict the performance of the proposed solar house. A solar chimney and a solid adsorption cooling cavity drove the natural ventilation. Their mathematical model results (without considering the cooling cavity) were validated with those obtained from the commercial model MIX2.0 (Multi-zone Infiltration and eXfiltration) developed by Li *et al.,* [22,23]. They found that the agreement between the two models was reasonable. Martı and Heras-Celemin [24] developed a dynamic model to investigate the performance of solar chimneys with thermal inertia. The authors validated their model results against experimental results and agreed with them [18,25]. Sakonidou *et al.,* [26] developed a mathematical model to determine the optimum inclination angle of the solar collector at which the maximum natural airflow inside the solar chimney can occur. They found that the maximum airflow was achieved at an optimum inclination angle of about 60° numerically and 65° to 76° mathematically. The model validation showed a good agreement between CFD and experimental results.

2. Solar Chimney Concept for Cabin Soak Temperature Reduction

As shown in Figure 1, the solar chimney system will create a hotspot zone to work as a thermal force device to maximize the air temperature difference between the solar-induced ventilation system and the car cabin to induce a natural convective air stream that can flow from the ambient passing through the car cabin and discharge to the surrounding through the solar chimney. In addition, its channel height will provide the required height for sufficient stack pressure to improve the airflow rate.

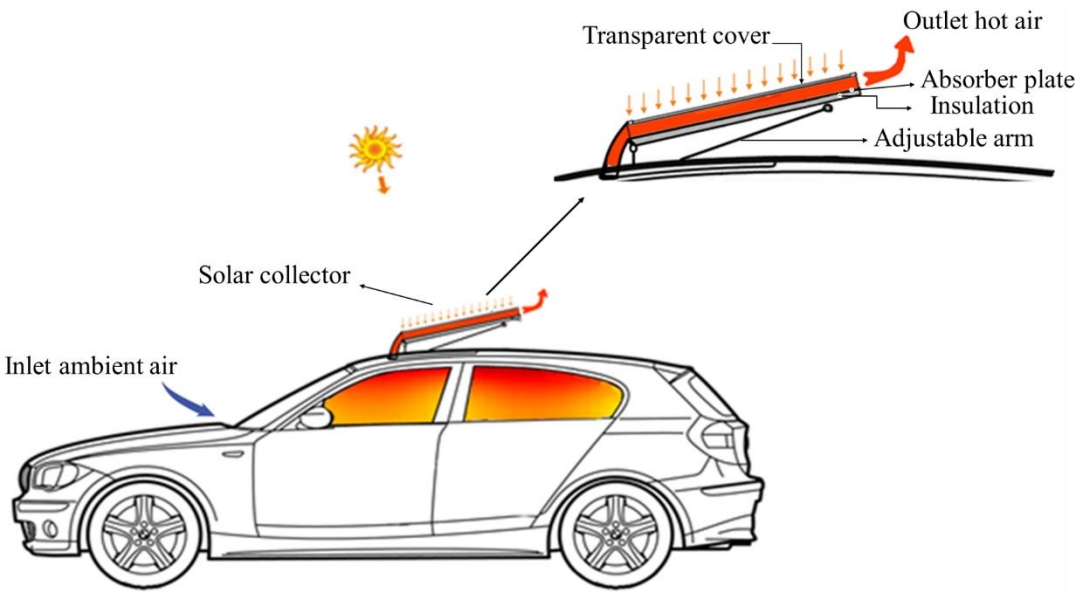

Fig. 1. Schematic diagram of solar chimney attached to the car cabin

2.1 System Description

The scheme of the system considered is sketched in Figure 1. The dimensions and physical characteristics of the system correspond to studied solar chimney values and with experimental data published by Lahimer *et al.,* [4]. The solar air collector system consists of an enclosure, a single glass, an absorber made of black metallic, and insulations [6,18,25,27,28].

3. Mathematical Model Development

The mathematical equations will be based on heat and mass transfer fundamentals and solar engineering calculations. Then, the model results will be validated with the theoretical and experimental results.

3.1 Design Assumptions

The following assumptions are based on experimental and theoretical studies [5,18,25,27-30]:

(i) One-dimensional heat transfer mode, steady-state conditions, and laminar flow are assumed.
(ii) Car cabin temperature is considered to be uniform.
(iii) The cover is assumed to be opaque to infrared radiation, and its energy absorbability of solar radiation is negligible.
(iv) Frictional losses along the collector surfaces have a minor effect due to very low-velocity flow compared to the pressure drops at the inlet and outlet openings, which can be neglected in this model.
(v) All thermos-physical properties of the fluid are constant and function of temperature; they are assessed at an average temperature in the range of 293 K<T_f<333 K.
(vi) It is assumed that the walls of the vertical stack are adiabatic.
(vii) The thermal capacities of the glass cover, absorber plate and temperature drop across them are negligible.
(viii) Glass (T_g) and absorber plate (T_p) surface temperatures are assumed to be uniform.

(ix) The solar collector chimney's top outlet and bottom input openings are assumed to be equal.
(x) Temperatures change only in the flow direction and are considered identical along the width.

3.2 Thermal Network

The heat transfer processes are shown in Figure 2. These processes can be represented by a thermal network (Figure 3) [25].

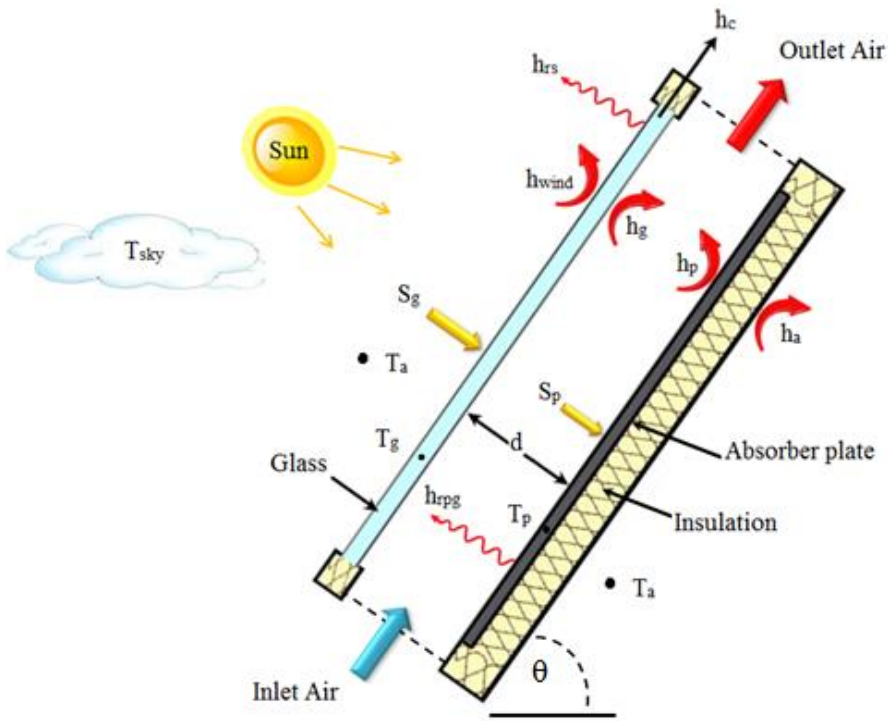

Fig. 2. Schematic diagram of the heat transfer in the physical model

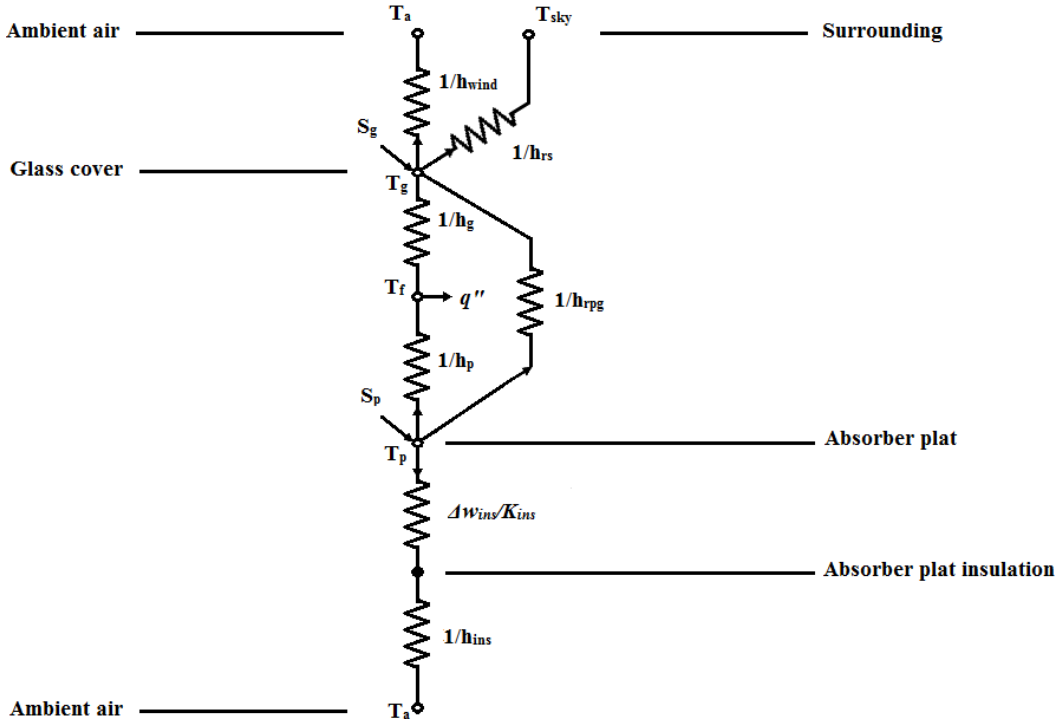

Fig. 3. System thermal network

3.3 Energy Balance Equations

This model is designed based on the energy balance analysis to predict the absorber plate, the air in the flow channel, and glass cover temperatures of a solar-induced cooling system and the induced flow rate.

3.3.1 Energy balance equation for glass cover

The energy balance equations for the glass cover can be written as:

[Incident solar radiation] + [radiative heat gain by glass cover from absorber plate] = [convective heat loss to air in the flow channel] + [overall heat loss coefficient from glass to ambient].

Mathematically, it can be formulated as:

$$S_g A_g + h_{rpg} A_p (T_p - T_g) = h_g A_g (T_g - T_f) + U_t A_g (T_g - T_a) \quad (1)$$

The above equation can be rearranged as:

$$(h_g A_g + h_{rpg} A_p + U_t A_g) T_g - h_g A_g T_f - h_{rpg} A_p T_p = S_g A_g + U_t A_g T_a \quad (2)$$

(a) Heat transfer from glass cover to ambient

The overall heat loss coefficient from the glass cover to the ambient (U_t) is the summation of radiative loss to the sky, convective loss due to wind, and conduction through glass. It can therefore be written as follows:

$$U_t = h_{rs} + h_{wind} + h_c \tag{3}$$

(i) The radiative heat transfer coefficient

The radiative heat transfer coefficient from the outer glass surface to the sky, referred to as the ambient temperature (h_{rs}), is given by Eq. (4) [31,32]:

$$h_{rs} = \frac{\sigma\varepsilon_g (T_g + T_{sky})(T^2{}_g + T^2{}_{sky})(T_g - T_{sky})}{(T_g - T_a)} \tag{4}$$

The sky temperature can be calculated using one of the several available correlations, it can be roughly calculated $T_{sky} = T_a - 6$ or $T_{sky} = T_a - 9$ [31,33,34]. In contrast, some researchers took it simply equal to the ambient temperature $T_{sky} = T_a$ [35]. In this analysis, the implemented sky temperature is $T_{sky} = 0.0552 T_a{}^{1.5}$, this relation is obtained by Swinbank [36], T_{sky} and T_a are both in Kelvin.

(ii) The convective heat transfer coefficient

The convective heat transfer coefficient between the glass cover surface and the ambient air is due to wind; it is determined with respect to the wind velocity (V) as:

$$h_{wind} = 2.8 + 3.0V \tag{5}$$

V is the wind speed over the surface (for $0 \leq V \leq 7$ m/ s). It is a linear empirical formula developed by Watmuff *et al.,* [37] for natural flow convection. These formulae are reported by several authors and used in many studies [5,27,28,38-41]. Khoukhi *et al.,* [42] used the above formulae at a wind speed velocity of 1.5 m/s, while Akhtar and Mullick [29] found by the analysis that a 10% error in the value of h_{wind} led to 1–2% error in the value of U_t. So, Watmuff's correlation h_{wind} will be employed in this article unless otherwise stated. However, for simplicity, the conductive heat transfer coefficient for glass h_c can be taken as (5.91 W/m^2 K) [5,28].

(b) Solar radiation heat flux

The absorption of solar radiation heat flux in the glass cover S_g is given by:

$$S_g = \alpha_g I_t \tag{6}$$

α_g = Glass absorptivity is 0.06 [12,28].
I_t = Total solar radiation on a tilted surface (W/m^2).

3.3.2 Energy balance equation for the air between the glass cover and absorber plate

The energy balance for the air in the gap between the glass cover and absorber plate is as follows:

[Convective heat transfer from the absorber plate to the air] + [convective heat transfer from the glass to the air] = [useful heat gain by the air].

This energy balance can mathematically be formulated as:

$$h_p A_p (T_p - T_f) + h_g A_g (T_g - T_f) = q'' \tag{7}$$

The equation below can be used to calculate the heat removal (useful heat gain) by the air stream (q'') [43]:

$$q'' = mC_{f1}(T_{fo} - T_{fi}) \tag{8}$$

The average air temperature (T_f) for the air in the gap can be calculated using a simple linear equation based on experimental observations [18]. It is given as in Eq. (9):

$$T_f = \gamma T_{fo} + (1-\gamma) T_{fi} \tag{9}$$

A value of 0.75 is taking for γ as assumed by Hirunlabh *et al.,* [18]. T_{fi} is assumed to be equal to the car cabin temperature (T_c). Hence, the heat removal by the air between the glass and absorber plate can be written as:

$$q'' = \frac{mC_{f1}(T_f - T_c)}{\gamma} \tag{10}$$

Therefore, by substituting the value of q'' in Eq. (7) and rearranging it, the energy balance for the air between the glass and absorber plate can be written as in Eq. (11):

$$h_g A_g T_g - (h_g A_g + h_p A_p + \frac{mC_{f1}}{\gamma}) T_f + h_p A_p T_p = -(\frac{mC_{f1}}{\gamma}) T_c \tag{11}$$

3.3.3 Energy balance equation for the absorber plate

The energy balance equation for the absorber plate can be written as:

[Incident solar radiation] = [convective heat loss to air in the flow channel] + [radiative heat loss to the glass cover] + [conduction to the ambient].

Mathematically, it can be formulated as:

$$S_p A_p = h_p A_p (T_p - T_f) + h_{rpg} A_p (T_p - T_g) + U_b A_p (T_p - T_a) \tag{12}$$

By rearranging the above equation, we obtain:

$$-h_{rpg} A_p T_g - h_p A_p T_f + (h_p A_p + h_{rpg} A_p + U_b A_p) T_p = S_p A_p + U_b A_p T_a \tag{13}$$

A_g, A_p is assumed to be equal. h_{rpg}, h_p, U_b, and S_p can be calculated from the below-given relations.

The overall back heat transfer coefficient U_b from the bottom of the absorber plate to the ambient is given by Klein [44]:

$$U_b = \frac{1}{\frac{1}{h_{ins}} + \frac{\Delta w_{ins}}{k_{ins}}} \tag{14}$$

To some extent, it is reasonable to consider that all resistance to heat flow is due to insulation. Thus, convection and radiation resistance to the surrounding can be neglected [45]. The above equation can be written as (15):

$$U_b = \frac{k_{ins}}{\Delta w_{ins}} \tag{15}$$

(a) Absorbed solar radiation on the absorber plate

The incident solar radiation flux passing through the glass cover is absorbed by the absorber plate and given by:

$$S_p = \tau_g \alpha_p I_t \tag{16}$$

Where glass transmitivity τ_g is taken as 0.84 and absorptivity of the absorber plate α_p as 0.95 [12,28].

3.4 Heat Transfer Coefficients

The above energy balance equations consist of heat transfer coefficients; h_{rpg}, h_g and h_p; below are their related equations:

3.4.1 The radiative heat transfer coefficient between absorber plate and glass cover

The radiative heat transfer coefficient between the absorber plate and the glass cover (h_{rpg}) is given by Eq. (17) [31,32,46]:

$$h_{rpg} = \frac{\sigma(T_g{}^2 + T_p{}^2)(T_g + T_p)}{\frac{1}{\varepsilon_g} + \frac{1}{\varepsilon_p} - 1} \tag{17}$$

3.4.2 Convective heat transfer coefficient between the glass cover and the air in the flow channel

The empirical relations and correlations used to calculate the natural convective heat transfer coefficients and the Nusselt number (*Nu*) of natural convection on inclined plates for laminar flow are obtained from Holman [32]:

$$h_g = \frac{NuK_f}{L_g} \tag{18}$$

Nusselt number

$$Nu = 0.60\ (Gr_x\ \cos\theta\,\mathrm{Pr})^{0.2} \qquad 10^5 \langle Gr\,\mathrm{Pr} \langle 10^{11}$$

Grashof number,

$$Gr = \frac{g\beta S_g (L_g)^4}{K_f \upsilon_f{}^2}$$

and Prandtl number,

$$Pr = \frac{\mu_f C_f}{K_f}$$

(i) Physical properties of air

Air thermal properties are assumed to vary linearly with the air temperature and evaluated at mean film temperatures of the average surface and air temperatures [20]. The correlations given below were proposed by Ong [20] and based on tabulated data from Incropera *et al.,* [47] for air properties between 300K and 350K.

$$\beta = \frac{1}{T_m}$$

$$T_m = \frac{T_f + T_S}{2}$$

where T_s represents the surface average temperature, it is equal to T_g when the glass cover is considered and equal to T_p when the absorber plate is considered.

$$T_m = \frac{(T_g + T_f)}{2}$$

Thermal conductivity:

$$K_f = 0.0263 + 0.000074 \quad (T_m - 300)$$

Kinematic viscosity

$$\upsilon_f = \frac{\mu_f}{\rho_f}$$

Dynamic viscosity:

$$\mu_f = [1.846 + 0.00472(T_m - 300)] \times 10^{-5}$$

Specific heat:

$$C_f = [1.007 + 0.00004(T_m - 300)] \times 10^{3}$$

Density:

$$\rho_f = [1.1614 - 0.00353(T_m - 300)]$$

3.4.3 Convective heat transfer coefficient between the absorber plate and the air in the flow channel

The calculation of the convective heat transfer coefficient between the absorber plate and the air in the flow channel is given below:

$$h_p = \frac{Nu_1 K_{f1}}{L_p} \tag{19}$$

$$Nu_1 = 0.60\,(Gr_{x1} \cos\theta \,\mathrm{Pr}_1)^{0.2}$$

Grashof number,

$$Gr_1 = \frac{g\beta_1 S_p (L_p)^4}{K_{f1} \upsilon_{f1}^{\,2}}$$

and Prandtl number,

$$\Pr_1 = \frac{\mu_{f1} C_{f1}}{K_{f1}}$$

$$\beta_1 = \frac{1}{T_{m1}}$$

$$T_{m1} = \frac{(T_p + T_f)}{2}$$

$$K_{f1} = 0.0263 + 0.000074\,(T_{m1} - 300)$$

$$\upsilon_{f1} = \frac{\mu_{f1}}{\rho_{f1}}$$

$$\mu_{f1} = [1.846 + 0.00472\ (T_{m1} - 300)] \times 10^{-5}$$

$$C_{f1} = [1.007 + 0.00004\ (T_{m1} - 300)] \times 10^{3}$$

$$\rho_{f1} = [1.1614 - 0.00353\ (T_{m1} - 300)]$$

Those empirical equations also apply to extensive applications such as solar chimney power plants within the above operating temperature [48].

3.5 Mass Air Flow Rate through Solar Chimney and Stack

The required air mass flow rate (kg/s) through the solar chimney is caused only by the buoyancy force. It can be estimated according to thermodynamics, fluid dynamics theories, and the energy conservation law applied to the car cabin. Once known, the solar chimney's parameters can be designed to induce the required air mass flow rate that can carry out the heat gain by the car cabin.

3.5.1 Natural draft driving forces

A natural draft is the upward displacement of the hot air, replacing it with cold fresh air. The flow can be induced by buoyancy force resulting from the density difference between interior and exterior air caused by the temperature difference between the space and its surroundings. To ensure the flow, a draft or buoyancy force has to overcome the gravitational force and frictional loss in the two openings and duct [49-51]. Accordingly, if the indoor possesses a higher temperature than the environment, hot air (less dense) will move up and skip from the top opening and let the cold air enter from the lower opening [52]. Only pressure due to stack is going to be considered.

$$\Delta P_t = \Delta P_w + \Delta P_s \tag{20}$$

where,

ΔP_t = Total driving pressures difference (Pa)
ΔP_w = Pressures difference due to Wind (Pa)
ΔP_s = Pressures difference across the opening (Pa), due to stack effect or temperature forces

(a) Buoyancy force

The pressure drops of the stack effect available to withdraw the air through the duct can be calculated with the equations presented below [23,53].

The pressure resulted by the buoyancy force, ΔP_s is obtained by below integration:

$$\Delta P_s = P_i - P_o = \mathrm{g}\int_0^h (\rho_o - \rho_i)dh \tag{21}$$

where,

ΔP_s = Stack pressure (Pa)
P_i = Static pressure at the inlet (Pa)
P_o = Static pressure at outlet (Pa)
ρ_o = Density of the outside air (kg/m^3)
ρ_i = Density of the inlet air to the chimney (kg/m^3), same as ρ_f. Commonly ρ_i is assumed to be constant within the chimney or to vary linearly with height [54].
g = Gravitational constant, (9.81m/s^2)
h = Stack height of the chimney channel, (m)

Since air is considered a perfect gas, the relationship between pressure, density, and temperature is expressed as [50];

$$P = \rho RT$$

where R is the gas constant for the air with value of 287J kg^{-}1 K^{-}1.

The above equation can be shown in terms of temperature [50,52]:

$$\Delta\rho = \frac{P_o}{RT_o}\left(\frac{T_i - T_o}{T_i}\right) = \rho_o\frac{\Delta T}{T_i} = \rho_i\frac{\Delta T}{T_o}$$

From Figure 4, the pressure difference between points (a) and (*i*) can be derived:

$$\Delta P_s = P_\mathrm{a} - P_i = P_b + \rho_o \mathrm{g}h - P_b - \rho_i \mathrm{g}h$$

$$\Delta P_s = \mathrm{g}h(\rho_o - \rho_i) = \mathrm{g}h\Delta\rho = \frac{\rho_o \mathrm{g}h\Delta T}{T_i} = \frac{\rho_i \mathrm{g}h\Delta T}{T_o} \tag{22}$$

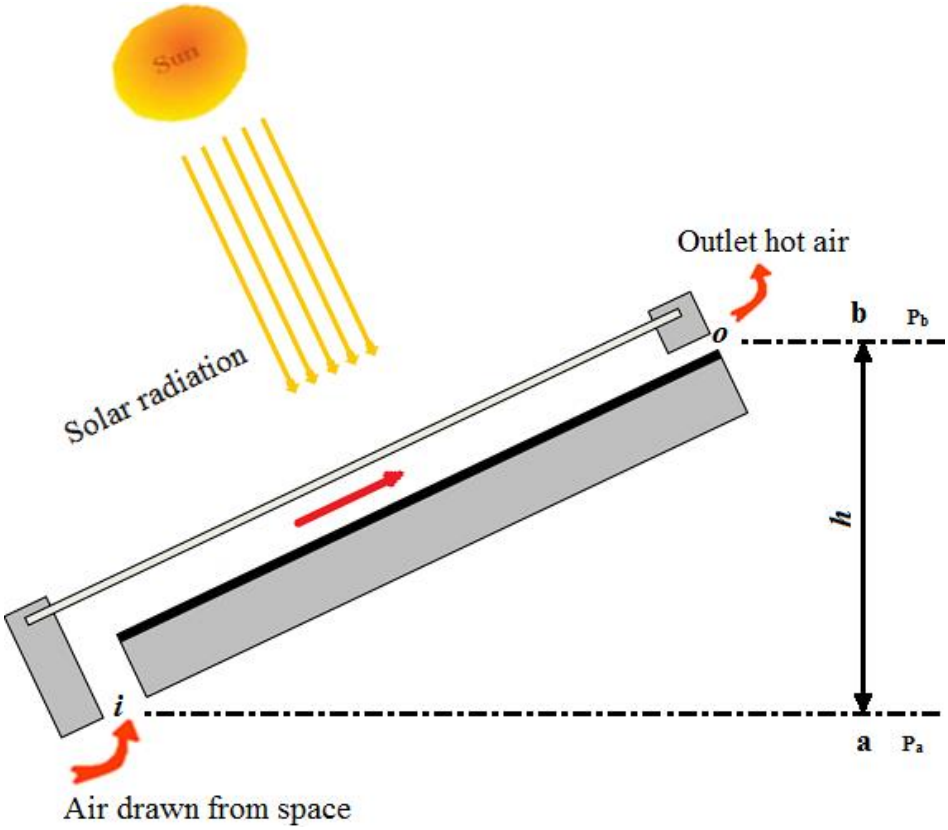

Fig. 4. Schematic diagram of the naturally induced ventilation through the solar chimney

Similarly, Andersen [50] used a momentum equation based on Newton's second law to find the linear pressure distribution between the openings. Thus, the pressure difference generated by the difference in temperature between the air inside and outside may be expressed as:

$$\Delta P_s = P_i - P_o = gh(\rho_o - \rho_i) = gh\Delta\rho = \frac{\rho_o gh\Delta T}{T_i} = \frac{\rho_i gh\Delta T}{T_o}$$

$$\Delta P_s = \rho_i gh\frac{\Delta T}{T_o}$$

$$\Delta P_s = P_i - P_o = \rho_i gh\frac{Ti-To}{To}$$

However, for an inclined chimney, h=Lsinθ.

where,

P_i = Pressure at the inlet, (Pa)
P_o = Pressure at the outlet, (Pa)
T_i = Inside chimney temperature, (°C)
T_o= Outside chimney temperature, (°C)
L = Length of the duct, (m)
ϑ = Inclination of the duct axis to horizontal, (°)

When $T_i > T_o$, an upward flow occurs and a reverse flow occurs when $T_i < T_o$.

The buoyancy pressure can be defined as the difference between the pressure exerted by the weight of a column of air in the chimney at temperature T_i and the pressure exerted by an equivalent column of outside air at temperature T_o [55].

The pressure difference that drives airflow through a stack due to buoyancy force can be expressed in different relationships. For example [56]:

$$\Delta P_s = -3455\Delta h(\frac{1}{T_o + 273} - \frac{1}{T_i + 273})$$

where,

ΔP_s = is the pressure difference at the stack inlet (when h=0) or the stack outlet (when h=stack height)
Δh = is the height difference between the openings (m)

3.5.2 Air mass flow rate equation

Based on the first law of thermodynamics along with the Bernoulli equation and conservation of mass using the continuity equation, a formula for the induced mass airflow rate by natural draft for the solar-induced ventilation system can be derived.

Bernoulli's equation, in general, is written as below:

$$P + \frac{1}{2}\rho v^2 + \rho gH = Constant \tag{23}$$

where,

v = Fluid flow velocity, m/s
g = Gravitational constant, 9.81m/s^2
H = Height of the point above a reference plane, m
P = Pressure at the chosen point, Pa
ρ = Density of the fluid at all points in the fluid, kg/m^3

Applying Bernoulli's equation between inlet *i* and outlet *o,* as shown in Figure 4, can get;

$$P_i + \frac{1}{2}\rho_i v_i^2 + \rho_i \mathrm{gH} = P_o + \frac{1}{2}\rho_o v_o^2 + \rho_o \mathrm{gH} \tag{24}$$

For the solar chimney with one inlet and one outlet openings the volume flow rate through each opening is given by:

$$Q = C_d A_o \sqrt{2\mathrm{g}h\frac{T_f - T_o}{T_o}} \tag{25}$$

The approximate amount of the rate of mass flow at the outlet of the solar air collector or at the vertical stack intake is [6,17]:

$$m = C_d \rho A_o \sqrt{\frac{2gL\sin\theta(T_f - T_c)}{(1+A_r^2)T_c}} \tag{26}$$

where,

m = Mass air flow rate, (kg/s)
C_d = Discharge coefficient of the channel opening, (0.6)
ρ = Air density in the duct, (kg/m^3)
A_i&A_o = cross sectional area of the inlet and outlet to airflow channel, (m^2)
L = Collector length, (m)
ϑ = Inclination of the collector axis to horizontal, (°)
T_f = Mean air temperature inside the airflow channel, (K)
T_c = Cabin temperature, K
A_r = Ratio of (A_o) to (A_i) $A_r = \frac{A_o}{A_i}$, is also known as an aspect ratio

For a given friction coefficient, the following formula for the airflow rate in ducts and chimneys can be used [55]:

$$Q = A_o \sqrt{2\frac{A_{eff}}{Pef\rho L}} \sqrt{\Delta P_s} \tag{27}$$

where,

A_{eff} = Effective area. This area is affected by opening size and configuration, cross-sectional area, and pressure losses.
Pe = Cross-sectional perimeter, (m)
f = Friction coefficient
ΔP_s = Pressure difference is the pressure difference between the interior and exterior at the height of the top opening and can be substituted by wind effects.

The interior mean air temperature of the extended vertical stack equals the mean air temperature (T_f) inside the airflow channel. However, the rate of mass flow at the extended vertical stack outlet can be estimated according to the following formula, taking into account that the total height will be the summation of the extended vertical stack height (H_{vst}) and airflow channel height ($L\sin\beta$) as in Yusoff *et al.,* [28]:

$$m = C_d \rho_f A_o \sqrt{\frac{2g(L\sin\theta + H_{vst})(T_f - T_c)}{(1+A_r^2)T_c}} \tag{28}$$

(a) Discharge coefficient

The coefficient of discharge (C_d) is defined as the ratio of the cross-section area at the vena contracta to the actual opening area [57]. It is considered an essential parameter to estimate the actual mass flow rate through the solar chimney when a theoretical model is employed to study the system's performance [58]. It considers the system's total flow resistances, the non-uniform

distribution of inlet velocities, the contraction of a fluid stream, surface roughness, among others [6,53,58].

$$C_d = \sqrt{\frac{1}{\sum K_i}}$$

where $\sum k_i$ is the sum of the pressure loss coefficient for the flow system [53].

A value of 0.57 can be considered as a typical value for thermal buoyant flows as suggested by Andersen [17] and used by several authors [5,25,26,28,57].

However, in case coefficient of velocity C_v and coefficient of contraction C_c are known, so C_d can be calculated [50]:

$C_d = C_v\, C_c$

3.6 Airflow Velocity

The velocity of air in the flow channel can be calculated using the Eq. (29) as suggested by Mathur and Mathur [5] and Ong and Chow [25]:

$$v_o = \frac{m}{\rho_f A_o} \tag{29}$$

v_o = velocity of the air at the outlet of the flow channel, (m/s)
ρ_f = Air Density (kg/m^3)
A_o = Outlet cross-sectional area to airflow channel, (m^2)

3.7 Solution Procedure

Since the three energy balance equations of the glass cover, air, and absorber plate are linear in T, they can be solved simultaneously using matrix inversion methods. Some researchers solve these matrices iteratively by using the Gauss-Seidel method employing a computer program such as FORTRAN [12]. The heat balance Eq. (30), Eq. (31), and Eq. (32) can be rearranged into a matrix form for the solution of those equations as:

$$(h_g A_g + h_{rpg} A_p + U_t A_g)T_g - h_g A_g T_f - h_{rpg} A_p T_p = S_g A_g + U_t A_g T_a \tag{30}$$

$$h_g A_g T_g - (h_g A_g + h_p A_p + \frac{mC_{f1}}{\gamma})T_f + h_p A_p T_p = -(\frac{mC_{f1}}{\gamma})T_c \tag{31}$$

$$-h_{rpg} A_p T_g - h_p A_p T_f + (h_p A_p + h_{rpg} A_p + U_b A_p)T_p = S_p A_p + U_b A_p T_a \tag{32}$$

$$a_1 T_g + b_1 T_f + c_1 T_p = R_1$$

$$a_2 T_g + b_2 T_f + c_2 T_p = R_2$$

$$a_3 T_g + b_3 T_f + c_3 T_p = R_3$$

$$\begin{bmatrix} a_1 & b_1 & c_1 \\ a_2 & b_2 & c_2 \\ a_3 & b_3 & c_3 \end{bmatrix} \begin{Bmatrix} T_g \\ T_f \\ T_p \end{Bmatrix} = \begin{Bmatrix} R_1 \\ R_2 \\ R_3 \end{Bmatrix} \tag{33}$$

where the matrix coefficients are defined as follows:

$$a_1 = h_g A_g + h_{rpg} A_p + (h_{win} + h_c + h_{rs}) A_g$$

$$b_1 = -h_g A_g$$

$$c_1 = -h_{rpg} A_p$$

$$a_2 = h_g A_g$$

$$b_2 = -(h_g A_g + h_p A_p + \frac{mc_{f1}}{\gamma})$$

$$c_2 = h_p A_p$$

$$a_3 = -h_{rpg} A_p$$

$$b_3 = -h_p A_p$$

$$c_3 = h_p A_p + h_{rpg} A_p + U_p A_p$$

The defined column vector terms in the right-hand side of the matrix form are as follows:

$$R_1 = \alpha_g A_g I_t + (h_{win} + h_c + h_{rs}) A_g T_a$$

$$R_2 = -\frac{mc_{f1}}{\gamma} T_c$$

$$R_3 = (\alpha_p \tau_g I_t) A_p + \frac{k_{ins}}{\Delta w_{ins}} A_P T_a$$

Eq. (33) can be writing as:

[A]x[T]=[R] (34)

Eq. (34) will have the solution as the temperature can be found by matrix inversion:

$[T]=[A]^{-1}x[R]$ (35)

Hence, temperature values of T_g, T_f, and T_p at specific iterations are obtained, and the air properties and heat-transfer coefficients are updated based on these temperatures [12]. Thus, the air mass flow rate can be calculated.

4. Results and Observations

4.1 Validation of the Developed Mathematical Model

Validation of the mathematical model will be performed by comparing the theoretical prediction results with those published in Lahimer *et al.,* [4] and Mathur and Mathur [5] and with the previous experimental work conducted by the authors of this paper. As a result, the system can be optimized and can then be constructed accordingly.

4.1.1 Model validation with Mathur and Mathur [5] study

The theoretical equations and procedures adopted in this study will be used to simulate the theoretical and experimental results of previous work in Mathur and Mathur [5] under the reference working conditions, assumptions, and materials properties.

The validation was carried out for the solar radiation and its corresponding ambient temperature under the range (500 to 750 W/m^2) with an increment of 50 W/m^2. The chimney was a unit square meter at a fixed inclination angle of 45°, chimney width 0.35 m, coefficient of discharge of air channel inlet (Cd=0.57), air gap (d=0.35) m, glass absorptivity (α_g=0.06), absorber plate absorptivity (α_p=0.95), glass emissivity (ε_g=0.90), absorber plate emissivity (ε_p=0.95), glass transmissivity (τ_g=0.84), mean temperature approximation coefficient (γ=0.74) and unit area ratio. In addition, the wind speed was not considered.

Figure 5(a) to Figure 5(c) show the variation of temperatures (T_g, T_f, and T_p) according to different solar radiation intensities and ambient temperatures.

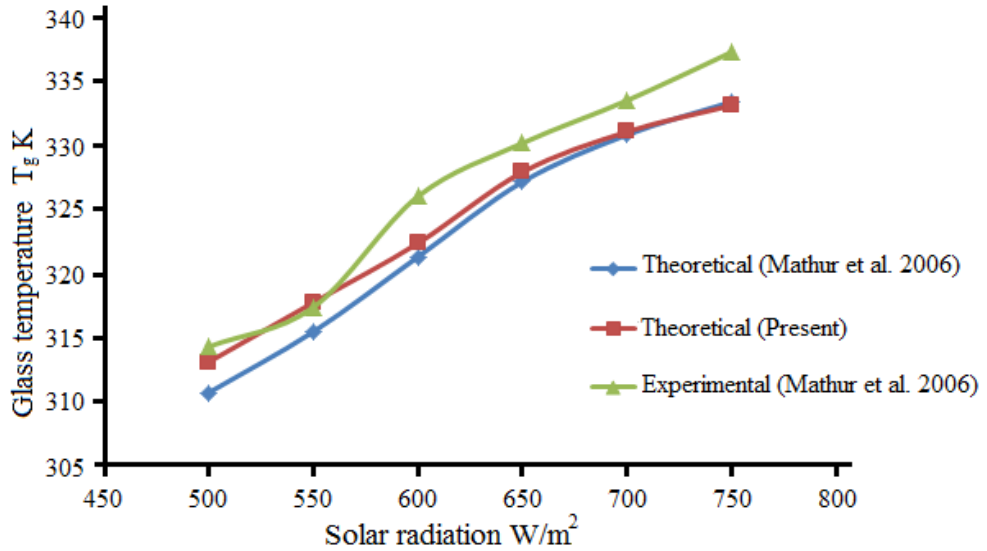

(a) Glass surface temperature

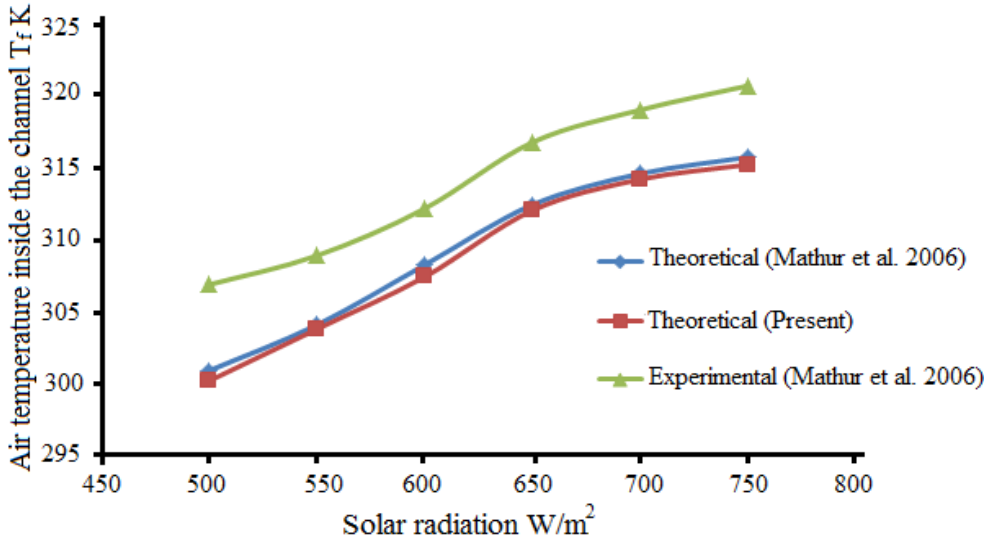

(b) The air temperature inside the airflow channel

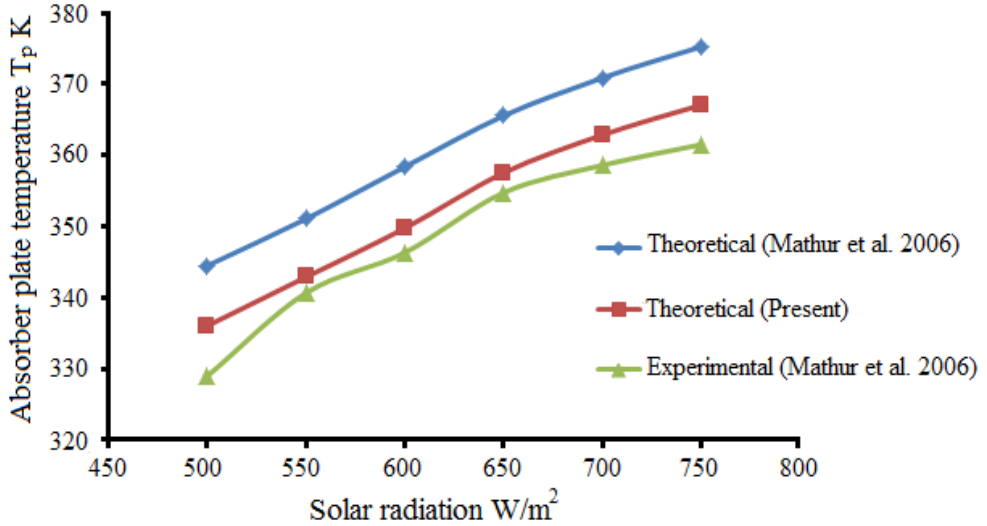

(c) Absorber temperature

Fig. 5. Comparison between the developed model results with theoretical and experimental results measured by Mathur and Mathur [5]

(a) Results discrepancy

The differences between the present model results and the numerical results of Mathur and Mathur [5] are due to simplifying assumptions made due to various weather conditions considered in the studies.

(b) Results analysis

Analysis of the above results indicates that all temperatures (glass, air, and absorber) and airflow gradually increase as the solar radiation intensity increases. The present model results are closer to the experimental results of Mathur and Mathur [5] than their numerical results. Thus, the difference between the predicted results of the current model and those in the literature is meager. However, the study of heat transfer in the chimney and investigating its performance using the mathematical model developed in this paper obtained through an overall energy balance on the solar chimney is consistent with the published literature and relatively more accurate.

For the glass, air, and absorber temperature, the value of R^2 (Coefficient of determination) is relatively high, which indicates a good fit between the literature and the present model. This study's theoretical result agrees well with the numerical and experimental findings, as documented by Mathur and Mathur [5].

Based on Figure 5 and Table 1, the statistical test results confirmed the accuracy of the theoretical model (present) with the theoretical results of Mathur and Mathur [5], consequently ensuring the appropriateness of the design and sizing assumptions and procedures being adopted in this study.

Table 1
Statistical test results of agreement between the developed theoretical model (present) and the theoretical of Mathur and Mathur [5]

Parameter	R^2	Efficiency
Glass temperature	0.999	0.97
Air temperature	0.998	0.99
Absorber temperature	0.999	0.513

4.1.2 Model validation with Lahimer et al., [4] experimental results

Although the developed model was validated against the theoretical and experimental results of Mathur and Mathur [5], the third check for the validity of this model will be performed against the experimental results conducted by the authors of this study to confirm the model's accuracy. The measurements (T_g, T_f, and T_p) were taken while conducting a soaking test to evaluate the system performance reported in a previous study of case (II) on June 6, 2017 [4]. Figure 6 to Figure 8 compare temperatures measured and model prediction results for that chosen date. The results of the theoretical model used for the comparison were obtained from the actual physical geometries: a 0.77m width and a 1.12 m collector length with an air gap of 0.1 m, with an aspect ratio of 11.2 (L/d=11.2).

The present model obtained several theoretical results, such as glass, absorber plate, and air in the chimney's channel temperatures, heat transfer coefficients, and air mass flow rate. In this study, the calculated temperatures are only the targets of this comparison with their recorded counterparts.

(a) Glass temperature

The theoretical model's glass temperature values are very close to those obtained experimentally. Also, the trends are almost identical, as shown in Figure 6.

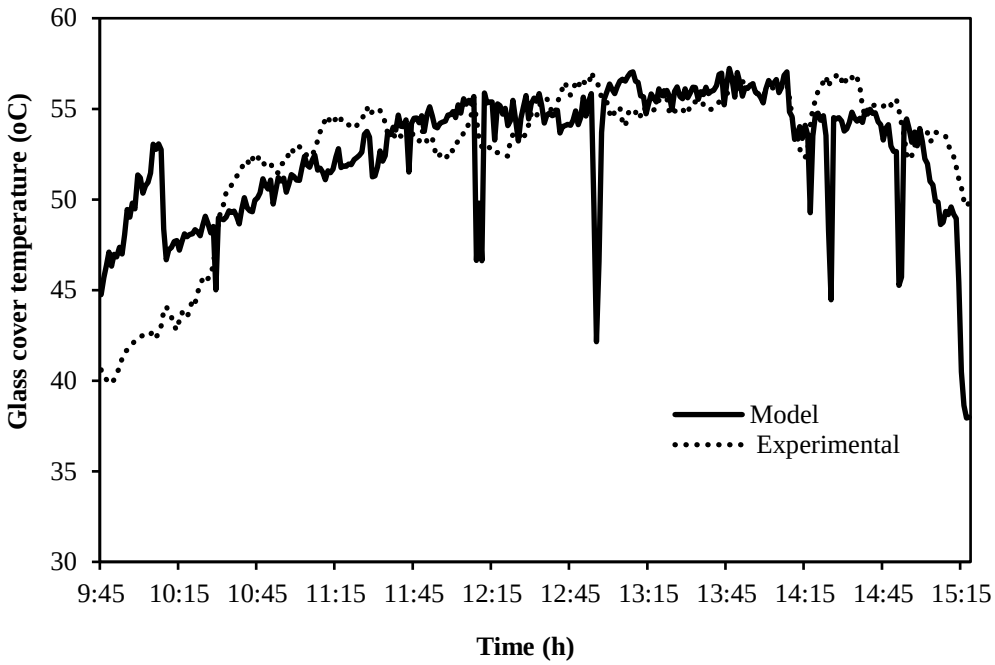

Fig. 6. Glass cover profiles for theoretically predicted data and experimental results

The average error was 0.4, which shows that the theoretical and experimental results are in good agreement with the glass temperature.

(b) Fluid temperature

Contrary to the glass cover temperature, it was observed from Figure 7 that the calculated temperatures of the air inside the solar chimney's channel typically are lower than the experimental temperature by an average of about 9.5%. However, both results experienced the same behavior during the comparison.

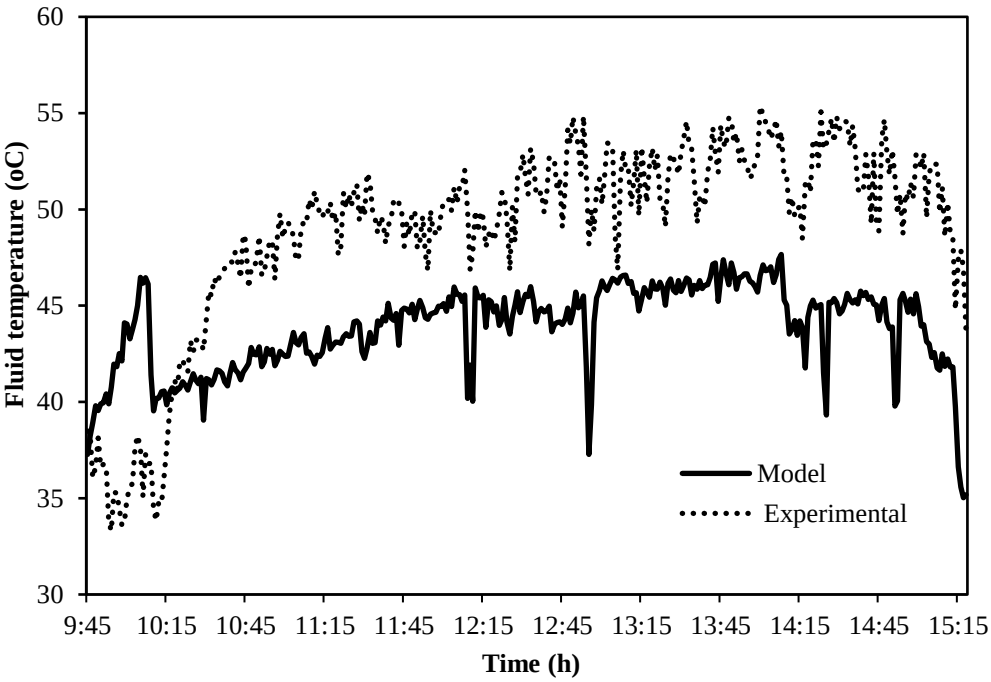

Fig. 7. Comparison of model and measured air temperature inside the solar chimney

According to Ong and Chow [25], the under-prediction of the temperatures of the air passing through the chimney's channel can be attributed to the exceeded heat gained experimentally by the air as it passes between two hot surfaces (glass and absorber plate). Therefore, the authors believed the theoretical model results could be enhanced by improving the heat transfer coefficient between the airflow, glass cover, and absorber plate.

Regardless of the assumptions driving the theoretical model, the primary variation driver, wind speed, is expected to enlarge the variation since it was estimated based on the forecast with an average value of 2 m/s.

(c) Absorber plate temperature

Figure 8 shows that the theoretical absorber plate surface temperatures were over-predicted, and the measured absorber plate surface temperature was lower than the theoretical temperature during the field test. Graphically, as shown in the figure, the temperature distribution pattern of the theoretical results is consistent with the experimental one. The sudden drop in the theoretical absorber plate temperature curve corresponded to the sudden reduction in solar irradiance. However, the experimental temperature measurements are typically 9.89% below the corresponding theoretical temperature, and the differences are apparent during peak solar irradiance hours.

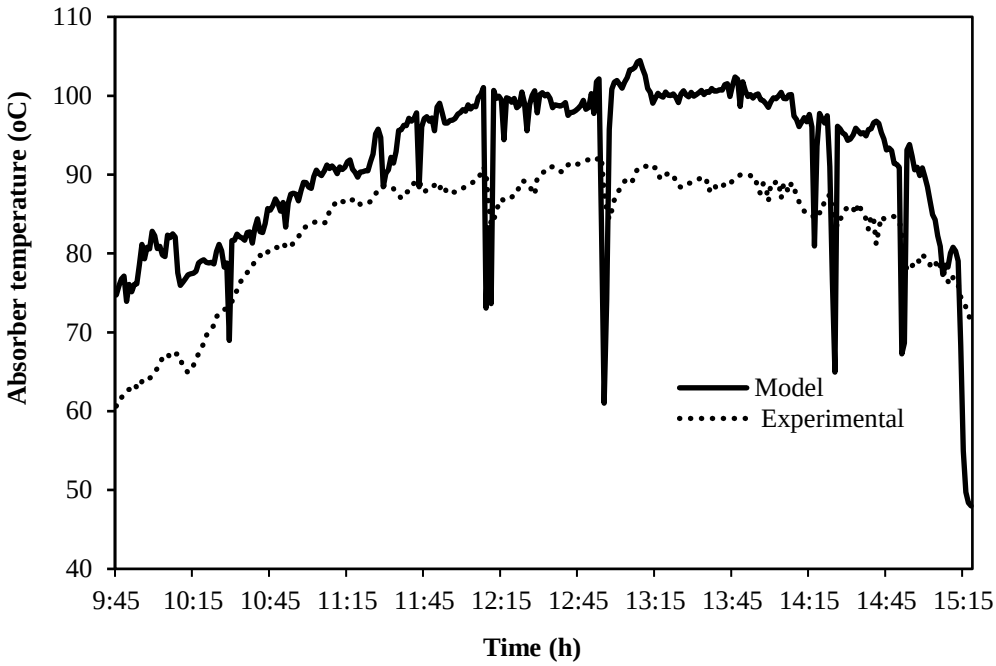

Fig. 8. Experimental and predicted absorber plate temperatures comparison

If the effect of the wind were included, the differences between the theoretical model and experimental results would be negligible because it was supposed to be a constant value in the model.

5. Conclusion and Future Work

A mathematical model for incorporating a solar chimney and vehicle cabin has been developed along with its solution procedure for energy analysis and parametric studies for obtaining the optimum geometries and performance for optimizing and designing the solar chimney. The main findings of this study are summarized below:

(i) The heat transfer mechanisms and the air mass flows in the two connected systems were successfully described by two coupled mathematical models.
(ii) Glass cover, air in the collector channel, and absorber plate temperatures are the core values of the developed model to predict the air mass flow rate through the collector channel and investigate the performance of solar-induced ventilation.
(iii) Glass, air, and absorbers are gradually increased with the solar radiation intensity increases.
(iv) Solar radiation is the major contributor to enhancing the performance of the solar-induced ventilation system.
(v) The glass temperatures obtained by the developed model were closer to the experiment results of both works than Mathur's model [5].
(vi) The air temperatures predicted by both models were below the measured values in both experiments.
(vii) The measured absorber temperatures in the literature were lower than both models' results, but the developed model's results are the closest to reality.
(viii) Although there are minor differences from the experimental results, the numerical results of the developed model demonstrated a better agreement with the experimental results than Mathur's model [5].

(ix) The value of R^2 for the glass, air, and absorber temperature is relatively high, indicating a good fit between the literature and the present model.

(x) The inconsistencies between the developed model and the experimental results could be attributed to factors not accounted for in the developed mathematical model such as the sky conditions, wind speed and direction, measurement uncertainty, and material properties.

(xi) The developed mathematical model can be used to study the influential parameters for the solar-induced ventilation system performance optimization and its components and gives comparable results to the experimental results.

The comprehensive analysis of the numerical results from the developed model showcased a significant level of agreement with both the experimental findings in the literature and the capabilities of the current model. Furthermore, it illuminated potential areas for future exploration, presenting researchers and automobile manufacturers with a broader perspective and a range of options for designing high-performance solar chimneys to enhance thermal comfort upon entering vehicles heated by the sun. Additionally, this study's developed model can be effectively utilized to predict the performance of any solar chimney and cabin air temperature for any parked vehicle.

Acknowledgement
The authors wish to express their acknowledgement to Universiti Malaysia Pahang under grant PGRS220388, as well as Solar Energy Research Institute (SERI), Universiti Kebangsaan Malaysia for providing the laboratory and testing facility.

References

[1] Chiou, J. P. "Application of solar-powered ventilator in automobiles." *SAE Transactions* (1986): 686-695. https://doi.org/10.4271/860585

[2] Jasni, Mohd Alif, and Faiza Mohamed Nasir. "Experimental comparison study of the passive methods in reducing car cabin interior temperature." In *Malaysia: International Conference on Mechanical, Automobile and Robotics Engineering (ICMAR) Penang*, pp. 229-233. 2012.

[3] Zulkifli, A. H., H. Nasution, A. A. Dahlan, and A. Abdul Aziz. "In-Cabin Vehicle Initial Temperature Control: A." *Journal of Advanced Review on Scientific Research* 13, no. 1 (2015): 1-8.

[4] Lahimer, A. A., K. Sopian, A. A. Razak, M. H. Ruslan, and M. A. Alghoul. "Experimental investigation on the performance of solar chimney for reduction of vehicle cabin soak temperature." *Applied Thermal Engineering* 152 (2019): 247-260. https://doi.org/10.1016/j.applthermaleng.2019.02.021

[5] Mathur, Jyotirmay, and Sanjay Mathur. "Summer-performance of inclined roof solar chimney for natural ventilation." *Energy and Buildings* 38, no. 10 (2006): 1156-1163. https://doi.org/10.1016/j.enbuild.2006.01.006

[6] Bansal, N. K., Rajesh Mathur, and M. S. Bhandari. "Solar chimney for enhanced stack ventilation." *Building and Environment* 28, no. 3 (1993): 373-377. https://doi.org/10.1016/0360-1323(93)90042-2

[7] Garg, H. P., and H. P. Garg. "Solar food drying." *Advances in Solar Energy Technology: Volume 3 Heating, Agricultural and Photovoltaic Applications of Solar Energy* (1987): 116-169. https://doi.org/10.1007/978-94-009-3797-0_3

[8] Das, S. K., and Yogender Kumar. "Design and performance of a solar dryer with vertical collector chimney suitable for rural application." *Energy Conversion and Management* 29, no. 2 (1989): 129-135. https://doi.org/10.1016/0196-8904(89)90021-6

[9] Ekechukwu, O. V., and B. Norton. "Design and measured performance of a solar chimney for natural-circulation solar-energy dryers." *Renewable Energy* 10, no. 1 (1997): 81-90. https://doi.org/10.1016/0960-1481(96)00005-5

[10] Vlachos, N. A., T. D. Karapantsios, A. I. Balouktsis, and D. Chassapis. "Design and testing of a new solar tray dryer." *Drying Technology* 20, no. 6 (2002): 1243-1271. https://doi.org/10.1081/DRT-120004050

[11] Barozzi, Giovanni Sebastiano, M. S. E. Imbabi, Enrico Nobile, and A. C. M. Sousa. "Physical and numerical modelling of a solar chimney-based ventilation system for buildings." *Building and Environment* 27, no. 4 (1992): 433-445. https://doi.org/10.1016/0360-1323(92)90042-N

[12] Bassiouny, Ramadan, and Nader SA Korah. "Effect of solar chimney inclination angle on space flow pattern and ventilation rate." *Energy and Buildings* 41, no. 2 (2009): 190-196. https://doi.org/10.1016/j.enbuild.2008.08.009

[13] Zhai, X. Q., Z. P. Song, and R. Z. Wang. "A review for the applications of solar chimneys in buildings." *Renewable and Sustainable Energy Reviews* 15, no. 8 (2011): 3757-3767. https://doi.org/10.1016/j.rser.2011.07.013

[14] Wang, Gang, Bing Chen, Mingsheng Liu, Joerg Henkel, and Stephan Raulin. "Analysis, design, and preliminary testing of solar chimney for residential air-conditioning applications." In *International Solar Energy Conference*, vol. 37475, pp. 291-297. 2004. https://doi.org/10.1115/ISEC2004-65093

[15] Abdallah, Amr Sayed Hassan, Hiroshi Yoshino, Tomonobu Goto, Napoleon Enteria, Magdy M. Radwan, and M. Abdelsamei Eid. "Integration of evaporative cooling technique with solar chimney to improve indoor thermal environment in the New Assiut City, Egypt." *International Journal of Energy and Environmental Engineering* 4 (2013): 1-15. https://doi.org/10.1186/2251-6832-4-45

[16] Zuo, Lu, Yuan Zheng, Zhenjie Li, and Yujun Sha. "Solar chimneys integrated with sea water desalination." *Desalination* 276, no. 1-3 (2011): 207-213. https://doi.org/10.1016/j.desal.2011.03.052

[17] Andersen, K. Terpager. *Theoretical considerations on natural ventilation by thermal buoyancy*. No. CONF-950624-. American Society of Heating, Refrigerating and Air-Conditioning Engineers, Inc., Atlanta, GA (United States), 1995.

[18] Hirunlabh, J., W. Kongduang, P. Namprakai, and J. Khedari. "Study of natural ventilation of houses by a metallic solar wall under tropical climate." *Renewable Energy* 18, no. 1 (1999): 109-119. https://doi.org/10.1016/S0960-1481(98)00783-6

[19] Afonso, Clito, and Armando Oliveira. "Solar chimneys: simulation and experiment." *Energy and Buildings* 32, no. 1 (2000): 71-79. https://doi.org/10.1016/S0378-7788(99)00038-9

[20] Ong, K. S. "A mathematical model of a solar chimney." *Renewable Energy* 28, no. 7 (2003): 1047-1060. https://doi.org/10.1016/S0960-1481(02)00057-5

[21] Dai, Y. J., K. Sumathy, R. Z. Wang, and Y. G. Li. "Enhancement of natural ventilation in a solar house with a solar chimney and a solid adsorption cooling cavity." *Solar Energy* 74, no. 1 (2003): 65-75. https://doi.org/10.1016/S0038-092X(03)00106-3

[22] Li, Yuguo, A. E. Delsante, and J. G. Symons. "Simulation tools for analysing natural ventilation of large enclosures with large openings." *AIRAH Journal* (1997).

[23] Li, Yuguo, Angelo Delsante, and Jeff Symons. "Prediction of natural ventilation in buildings with large openings." *Building and Environment* 35, no. 3 (2000): 191-206. https://doi.org/10.1016/S0360-1323(99)00011-6

[24] Martı, J., and M. R. Heras-Celemin. "Dynamic physical model for a solar chimney." *Solar Energy* 81, no. 5 (2007): 614-622. https://doi.org/10.1016/j.solener.2006.09.003

[25] Ong, K. S., and C. C. Chow. "Performance of a solar chimney." *Solar Energy* 74, no. 1 (2003): 1-17. https://doi.org/10.1016/S0038-092X(03)00114-2

[26] Sakonidou, E. P., T. D. Karapantsios, A. I. Balouktsis, and D. Chassapis. "Modeling of the optimum tilt of a solar chimney for maximum air flow." *Solar Energy* 82, no. 1 (2008): 80-94. https://doi.org/10.1016/j.solener.2007.03.001

[27] Maerefat, Mehdi, and A. P. Haghighi. "Passive cooling of buildings by using integrated earth to air heat exchanger and solar chimney." *Renewable Energy* 35, no. 10 (2010): 2316-2324. https://doi.org/10.1016/j.renene.2010.03.003

[28] Yusoff, Wardah Fatimah Mohammad, Elias Salleh, Nor Mariah Adam, Abdul Razak Sapian, and Mohamad Yusof Sulaiman. "Enhancement of stack ventilation in hot and humid climate using a combination of roof solar collector and vertical stack." *Building and Environment* 45, no. 10 (2010): 2296-2308. https://doi.org/10.1016/j.buildenv.2010.04.018

[29] Akhtar, N., and S. C. Mullick. "Approximate method for computation of glass cover temperature and top heat-loss coefficient of solar collectors with single glazing." *Solar Energy* 66, no. 5 (1999): 349-354. https://doi.org/10.1016/S0038-092X(99)00032-8

[30] Al-Kayiem, Hussain H., K. V. Sreejaya, and Syed Ihtsham Ul-Haq Gilani. "Mathematical analysis of the influence of the chimney height and collector area on the performance of a roof top solar chimney." *Energy and Buildings* 68 (2014): 305-311. https://doi.org/10.1016/j.enbuild.2013.09.021

[31] Duffie, John A., and William A. Beckman. *Solar energy thermal processes*. University of Wisconsin-Madison, Solar Energy Laboratory, Madison, WI, 1974.

[32] Holman, Jack Philip. *Heat transfer*. McGraw Hill, 1981.

[33] Whillier, A. "Design factors influencing solar collector performance in Low Temperature Engineering Application of Solar Energy." *ASHRAE, NYC* (1967).

[34] Luo, Weihong, Hendrik Feije de Zwart, Jianfeng DaiI, Xiaohan Wang, Cecilia Stanghellini, and Chongxing Bu. "Simulation of greenhouse management in the subtropics, Part I: Model validation and scenario study for the winter season." *Biosystems Engineering* 90, no. 3 (2005): 307-318. https://doi.org/10.1016/j.biosystemseng.2004.11.008

[35] Kumar, Suresh, and S. C. Mullick. "Glass cover temperature and top heat loss coefficient of a single glazed flat plate collector with nearly vertical configuration." *Ain Shams Engineering Journal* 3, no. 3 (2012): 299-304. https://doi.org/10.1016/j.asej.2012.03.008
[36] Swinbank, W. C. "Long-wave radiation from clear skies." *Quarterly Journal of the Royal Meteorological Society* 89, no. 381 (1963): 339-348. https://doi.org/10.1002/qj.49708938105
[37] Watmuff, J. H., W. W. S. Charters, and David Proctor. "Solar and wind induced external coefficients-solar collectors." *Cooperation Mediterraneenne pour l'Energie Solaire* (1977): 56.
[38] Duffie, John A., and William A. Beckman. *Solar engineering of thermal processes*. John Wiley & Sons, 1980.
[39] Agarwal, V. K., and D. C. Larson. "Calculation of the top loss coefficient of a flat-plate collector." *Solar Energy* 27 (1981): 69-71. https://doi.org/10.1016/0038-092X(81)90022-0
[40] Jain, Dilip. "Modeling the system performance of multi-tray crop drying using an inclined multi-pass solar air heater with in-built thermal storage." *Journal of Food Engineering* 71, no. 1 (2005): 44-54. https://doi.org/10.1016/j.jfoodeng.2004.10.016
[41] Khoukhi, Maatouk, and Shigenao Maruyama. "Theoretical approach of a flat plate solar collector with clear and low-iron glass covers taking into account the spectral absorption and emission within glass covers layer." *Renewable Energy* 30, no. 8 (2005): 1177-1194. https://doi.org/10.1016/j.renene.2004.09.014
[42] Khoukhi, M., S. Maruyama, and S. Sakai. "Non-gray calculation of plate solar collector with low iron glazing taking into account the absorption and emission with a glass cover." *Desalination* 209, no. 1-3 (2007): 156-162. https://doi.org/10.1016/j.desal.2007.04.025
[43] Sayigh, A. A. M., ed. *Solar energy engineering*. Academic Press, 1977.
[44] Klein, S. A. "Calculation of the monthly-average transmittance-absorptance product." *Solar Energy* 23, no. 6 (1979). https://doi.org/10.1016/0038-092X(79)90083-5
[45] Martín, R. Herrero, J. Pérez-García, A. García, F. J. García-Soto, and E. López-Galiana. "Simulation of an enhanced flat-plate solar liquid collector with wire-coil insert devices." *Solar Energy* 85, no. 3 (2011): 455-469. https://doi.org/10.1016/j.solener.2010.12.013
[46] Duffie, John A., and William A. Beckman. *Solar engineering of thermal processes*. Wiley, 1991.
[47] Incropera, Frank P., David P. DeWitt, Theodore L. Bergman, and Adrienne S. Lavine. *Fundamentals of heat and mass transfer*. Vol. 6. New York: Wiley, 1996.
[48] Zhou, Xinping, Jiakuan Yang, Bo Xiao, Guoxiang Hou, and Fang Xing. "Analysis of chimney height for solar chimney power plant." *Applied Thermal Engineering* 29, no. 1 (2009): 178-185. https://doi.org/10.1016/j.applthermaleng.2008.02.014
[49] Allard, Francis, and Cristian Ghiaus, eds. *Natural ventilation in the urban environment: assessment and design*. Routledge, 2012.
[50] Andersen, Karl Terpager. "Theory for natural ventilation by thermal buoyancy in one zone with uniform temperature." *Building and Environment* 38, no. 11 (2003): 1281-1289. https://doi.org/10.1016/S0360-1323(03)00132-X
[51] Hamdan, Mohammad O. "Analysis of a solar chimney power plant in the Arabian Gulf region." *Renewable energy* 36, no. 10 (2011): 2593-2598. https://doi.org/10.1016/j.renene.2010.05.002
[52] Germano, M., and C-A. Roulet. "Multicriteria assessment of natural ventilation potential." *Solar Energy* 80, no. 4 (2006): 393-401. https://doi.org/10.1016/j.solener.2005.03.005
[53] Gan, G., and S. B. Riffat. "A numerical study of solar chimney for natural ventilation of buildings with heat recovery." *Applied Thermal Engineering* 18, no. 12 (1998): 1171-1187. https://doi.org/10.1016/S1359-4311(97)00117-8
[54] Spencer, S., Z. D. Chen, Y. Li, and F. Haghighat. "Experimental investigation of a solar chimney natural ventilation system." In *Indoor Air: An Integrated Approach*, p. 813-818. Elsevier, 2000.
[55] Bouchair, Ammar. "Solar induced ventilation in the Algerian and similar climates." *PhD diss., University of Leeds*, 1989.
[56] Lush, D., K. Butcher, and P. Appleby. *Environmental Design: CIBSE Guide A*. Chartered Institute of Building Services Engineers, London (United Kingdom), 1999.
[57] Bassiouny, Ramadan, and Nader S. A. Koura. "An analytical and numerical study of solar chimney use for room natural ventilation." *Energy and Buildings* 40, no. 5 (2008): 865-873. https://doi.org/10.1016/j.enbuild.2007.06.005
[58] Arce, J., M. J. Jiménez, J. D. Guzmán, M. R. Heras, G. Alvarez, and J. Xamán. "Experimental study for natural ventilation on a solar chimney." *Renewable Energy* 34, no. 12 (2009): 2928-2934. https://doi.org/10.1016/j.renene.2009.04.026